

Numerical Simulation of Annular Flow Boiling in a Vertical Pipe Using Two-Fluid Model

Alen CUKROV*, Yohei SATO⁺, Ivanka BORAS*, Bojan NIČENO⁺

**Faculty of Mechanical Engineering and Naval Architecture, University of Zagreb,
Ivana Lučća 5, Zagreb, Croatia*

E-mails: alen.cukrov@fsb.hr, ivanka.boras@fsb.hr

*⁺Laboratory of Thermal Hydraulics, Paul Scherrer Institute, Villigen PSI,
Switzerland*

E-mails: yohei.sato@psi.ch, bojan.niceno@psi.ch

Abstract. *The goal of this paper is to develop a numerical model for computation of annular flow boiling in a vertical pipe under 70 bar pressure and 10 K inlet subcooling. The model is based on two-fluid formulation in conjunction with an extended formulation of Rensselaer Polytechnic Institute model for boiling flows. Here, the successful modeling of the annular flow boiling is achieved by use of closure correlations for interfacial transfer proposed by [1]. This refers to constitutive relations for vapor-bubble diameter and interfacial lift force, both being computed as flow regime dependent. A uniform wall heat flux is applied at the pipe wall, while the inlet mass fluxes were varied. The model validation is done by comparison of vapor volume fraction at specific points near the pipe outlet with the data extracted from measurements conducted by [2]. The obtained results agree well with the experimental data, thus indicating the reliability of the developed model in computation of such multiphase flow phenomena.*

1 Introduction

The annular pipe flow refers to a multiphase flow pattern where liquid film is present at the pipe wall, while the gas (or vapor) phase fills the core of the flow. The numerical modeling of this phenomena requires computationally expensive methods which are inconvenient to use in practice.

Thus, the goal of this work is to develop a numerical model which is able to accurately predict the flow fields in annular flow boiling regime with a reasonable computational cost. To this end, an Eulerian two-fluid model implemented in commercial CFD code ANSYS Fluent 18.1 is used.

The remainder of the paper is organized as follows. Chapter 2 introduces the mathematical formulation which is solved by the numerical procedure described in Chapter 3. The obtained results are given in Chapter 4. The paper ends with Chapter 5 where the main achievements are summarized.

2 Mathematical Model

2.1 Conservation Laws

Within the Eulerian two-fluid formulation, each phase is described by its own set of conservation equations. The interaction between the phases is established by interfacial exchange terms. Thus, the mass, momentum and energy equation read [3]

- conservation of mass

$$\frac{\partial}{\partial t}(\alpha_q \rho_q) + \nabla \cdot (\alpha_q \rho_q \vec{v}_q) = \sum_{p=1}^n (\dot{m}_{pq} - \dot{m}_{qp}) + S_q \quad (1)$$

- conservation of momentum

$$\begin{aligned} \frac{\partial}{\partial t}(\alpha_q \rho_q \vec{v}_q) + \nabla \cdot (\alpha_q \rho_q \vec{v}_q \vec{v}_q) = & -\alpha_q \nabla p + \nabla \cdot \bar{\bar{\tau}}_q + \alpha_q \rho_q \vec{g} \\ & + \sum_{p=1}^n (K_{pq}(\vec{v}_p - \vec{v}_q) + \dot{m}_{pq}\vec{v}_{pq} - \dot{m}_{qp}\vec{v}_{qp}) \\ & + (\vec{F}_q + \vec{F}_{lift,q} + \vec{F}_{vm,q} + \vec{F}_{td,q}) \end{aligned} \quad (2)$$

- conservation of energy

$$\begin{aligned} \frac{\partial}{\partial t}(\alpha_q \rho_q h_q) + \nabla \cdot (\alpha_q \rho_q \vec{u}_q h_q) = & \alpha_q \frac{\partial p_q}{\partial t} + \bar{\bar{\tau}}_q : \nabla \vec{u}_q - \nabla \cdot \vec{q}_q \\ & + S_q + \sum_{p=1}^n (Q_{pq} + \dot{m}_{pq}h_{pq} - \dot{m}_{qp}h_{qp}) \end{aligned} \quad (3)$$

In order to successfully model the annular flow boiling, an emphasis is put on treatment of lift force $\vec{F}_{lift,q}$ via lift force coefficient as well as on the interphase momentum exchange coefficient K_{pq} and the volumetric rate of the energy transfer between the phases Q_{pq} by influencing the computation of interfacial area.

2.2 Turbulence Model

Within this study, a mixture based two-equation RNG $k-\epsilon$ turbulence model with standard coefficients is used. Since the separation between the vapor phase and a liquid film is present in the annular flow boiling regime, the non-equilibrium wall functions are included in the model due to their ability to handle separated flows.

2.3 Boiling Model

The computation of flow boiling is accomplished by using an extended formulation of the well-established Rensselaer Polytechnic Institute (RPI) boiling model. The extension is realized by addition of extra terms in the wall heat partition equation together with inclusion of the liquid volume fraction function. Thus, the total wall heat flux reads [3]

$$\dot{q}_w = (\dot{q}_C + \dot{q}_Q + \dot{q}_E) f(\alpha_l) + (1 - f(\alpha_l)) \dot{q}_V + \dot{q}_G \quad (4)$$

where \dot{q}_C , \dot{q}_Q and \dot{q}_E are default RPI model's heat flux components consisted of convective, quenching and evaporative heat flux, respectively. The additional terms are the heat flux from wall to vapor \dot{q}_V and the heat flux from wall to any other gaseous phase present in the domain \dot{q}_G . Since the multiphase system within this case is composed of water and vapor, the latter term vanishes. These terms are defined on the basis of Newton's law of cooling and read [3]

$$\dot{q}_V = h_V (T_W - T_V) \quad (5)$$

$$\dot{q}_G = h_G (T_W - T_G) \quad (6)$$

where h_V and h_G are convective heat transfer coefficients and are computed from the wall function formulations [3].

Furthermore, the liquid volume fraction function $f(\alpha_l)$ reads [3]

$$f(\alpha_l) = \begin{cases} 1 - \frac{1}{2} e^{-20(\alpha_l - \alpha_{l,crit})} \\ \frac{1}{2} \left(\frac{\alpha_l}{\alpha_{l,crit}} \right)^{20\alpha_{l,crit}} \end{cases} \quad (7)$$

where the $\alpha_{l,crit}$ represents the critical value of the liquid fraction and is equal to 0.2.

In this study, the vapor temperature is considered constant and the mass transfer parameters were kept as default. Therefore, Tolubinski-Konstanchuk bubble departure diameter is retained together with frequency of bubble departure proposed by Cole, nucleation site density from Lemmert and Chawla and Delvalle-Kenning area influence coefficient.

2.4 Interfacial Transport

The mass, momentum and energy exchange between the phases is accomplished by the interfacial exchange terms in the governing equation set. Therefore, drag, lift, virtual mass and turbulent dispersion forces are taken into account in the momentum equation. These forces, except the lift force, are modeled using the models available in ANSYS Fluent 18.1. Thus, Ishii model is used for modeling the drag, virtual mass coefficient is retained 0.5 and constant, while Lopez de Bertodano model is used for modeling the turbulent dispersion force.

The lift force is modeled by using the lift coefficient correlation proposed by Yoon, Agostinelli and Baglietto [1] which reads

$$C_L = \begin{cases} 0.025, & \alpha_g \leq 0.25 \\ -0.025, & \alpha_g > 0.25 \end{cases} \quad (8)$$

This correlation is implemented within the framework of ANSYS Fluent 18.1 as a user-defined function (UDF).

Although the drag force is modeled using available Ishii formulation for boiling flows, the drag still could be influenced by assigning specific correlation for computation of interfacial area concentration. Thus, a correlation proposed by Yoon, Agostinelli and Baglietto [1] is used within this model and is defined as follows

$$a_{ij} = \frac{6\alpha_g}{d_s} \quad (9)$$

$$d_s = \begin{cases} 10.6 \left(\frac{p}{p_0} \right)^{-0.098} \sqrt{\left(\frac{\sigma}{\Delta \rho g} \right)} [\min(\alpha_g, 0.118)]^{0.35} & \alpha_g < 0.4 \\ 0.0019425 e^{(2.3637 \alpha_g)} & 0.4 < \alpha_g < 0.8 \\ 0.864 D_h & \alpha_g > 0.8 \end{cases} \quad (10)$$

The first expression (Equation 9) is well known particle model, while the second correlation (Equation 10) enables determination of the vapor-bubble diameter depending on the flow regime. These equations, in conjunction with the aforementioned lift coefficient correlation (Equation 8), play a key role in successful capturing of the annular flow patterns. Also, these expressions are implemented in ANSYS Fluent as UDF.

In addition, the turbulence interaction between the phases is modeled via Troshko-Hassan model, while Ranz-Marshall model is used for modeling the interfacial heat transfer.

3 Numerical Method

3.1 Description of the Case and Geometry

The flow domain is considered as 2D axisymmetric as shown in Figure 1. The mesh is generated using Gmsh [4], an open source mesh generation software. The computational mesh consists of 2300 cells.

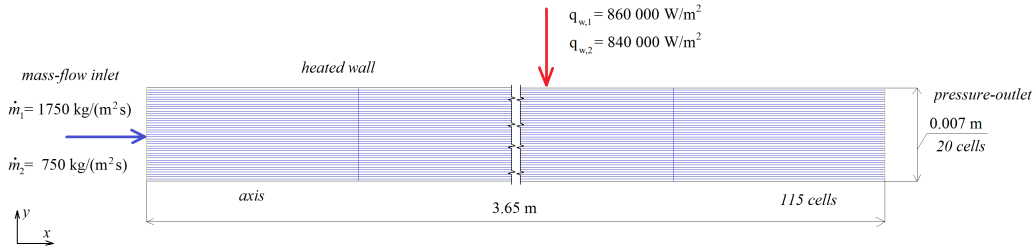


Figure 1: Computational domain with the assigned boundary values.

The flow conditions in the domain are defined upon the experiments carried out by Adamsson [1]. The operating pressure is 7 MPa, and 10 K sub-cooled liquid enters the

domain. The computations were performed for the lowest and the highest mass flux in experiment, $750 \text{ kg}/(\text{m}^2 \text{ s})$ and $1750 \text{ kg}/(\text{m}^2 \text{ s})$, respectively. In both simulations, a uniform wall heat flux is applied at pipe wall. In simulation with the lowest mass flux, the wall heat flux is set to $840 \text{ kW}/\text{m}^2$. This value is chosen according to mean heat flux in the experiment with the lowest mass flux and uniform power distribution. On the other hand, in simulation with the highest mass flux, a uniform wall heat flux of $860 \text{ kW}/\text{m}^2$ is applied. This value is mean heat flux in experiment with the highest mass flux and inlet-peaked power profile. Since there was no explicit information about the heat flux within the case of uniform heat flux and the mass flux of $1750 \text{ kg}/(\text{m}^2 \text{ s})$, this value is used as boundary condition. Under these conditions, the annular flow occurs in the pipe. The vapor is assumed to remain at saturation temperature, and its generation is induced by the applied heat flux. Therefore, a zero-value of volume fraction field is defined at the domain's inlet.

Table 1: Physical properties of the phases.

	Water	Vapor
Density, kg/m^3	741.4	36.2
Specific heat capacity at constant pressure, $\text{J}/(\text{kg K})$	5389	5325
Thermal conductivity, $\text{W}/(\text{m K})$	0.5731	0.0627
Dynamic viscosity, $\text{kg}/(\text{m s})$	$9.16 \cdot 10^{-3}$	$1.89 \cdot 10^{-5}$
Molecular weight, kg/kmol	18.0152	
Standard state enthalpy, $\text{J}/(\text{kg mol})$	0	$2.72 \cdot 10^7$
Reference temperature, K	298.15	298.15

The physical properties of water and liquid are taken from [5] and assumed to be constant. Table 1 summarizes the physical properties used in computation.

3.2 Numerical Solution

The equations are solved using finite volume method implemented in commercial CFD code ANSYS Fluent 18.1. The equations are discretized using first-order upwind discretization scheme. The coupling between the pressure and velocity is done using *Coupled* scheme available in ANSYS Fluent in conjunction with *Coupled with Volume Fraction* option.

The computations were started as transient and were performed in seven stages, six transient and one steady state. Each of transient stages consisted of 100 iterations with 50 iterations within single time step. Firstly, 100 iterations with a time-step of $1\text{e-}9 \text{ s}$ were performed with 50 iterations in each time step. After this is done, the next 100 iterations with the time-step of $1\text{e-}7 \text{ s}$ were performed, also with 50 iterations in a step.

Then, this procedure is repeated for the time steps: 1e-5 s, 1e-4 s, 1e-3 s and finally 1e-2 s. In the last transient computation, with the time step of 1e-2 s, the under-relaxation factors were increased as shown in Figure 2. After the solution convergence is reached, 2000 steady state iterations were performed. The value of Courant number was set to 4 in all simulations, while the initial field values were computed from domain's inlet.

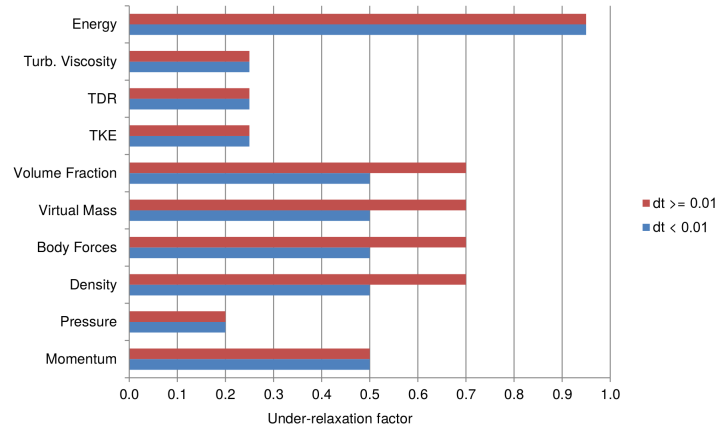


Figure 2: The under-relaxation factors applied during solution process.

The choice of under-relaxation factors was based on the recommendations given in ANSYS Fluent documentation [3] and findings reported in the thesis of Fincher [6].

4 Results

In addition to monitoring the residual values, the solution convergence is tracked by two additional flow quantities: global mass balance and average outlet vapor fraction [7]. The solution is converged when these quantities reach constant value.

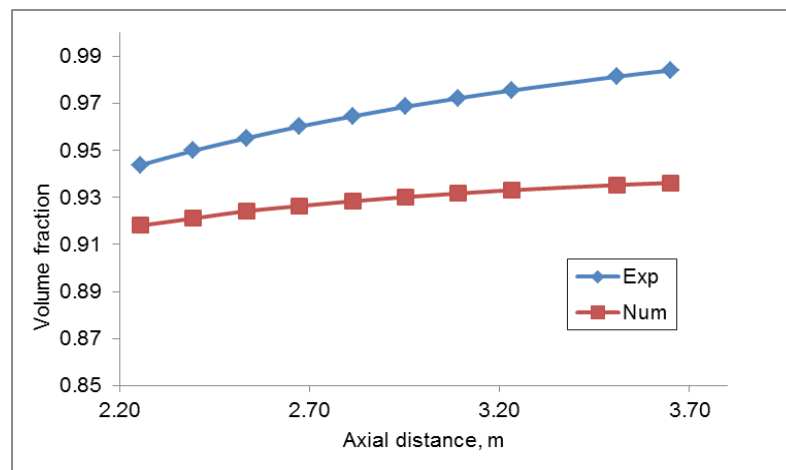


Figure 3: Axial void fraction distribution in the case with the mass flux 750 kg/(m²s).

The data provided by experiments are the mass flow rates of vapor, liquid film and liquid droplets. The exact numerical values of these quantities are extracted from plots using WebPlotDigitizer [8]. The vapor volume fraction is computed on the basis of the experimentally obtained mass flow values, using the following expression

$$\alpha_v = \frac{\frac{\dot{m}_{vapor}}{\rho_{vapor}}}{\frac{\dot{m}_{vapor}}{\rho_{vapor}} + \frac{\dot{m}_{droplet}}{\rho_{liquid}} + \frac{\dot{m}_{film}}{\rho_{liquid}}} . \quad (11)$$

Figure 3 shows the axial distribution of vapor volume fraction in comparison with experimental results. The highest error occurs at the outlet section and has a value of 4.9 %. The distribution of vapor volume fraction at axial distances from ca. 0.75 to ca. 0.9 m from domain's inlet is depicted in Figure 4. At the top of the figure, the volume fraction at the center of the pipe is higher than that in the near wall region, featuring the annular boiling regime.

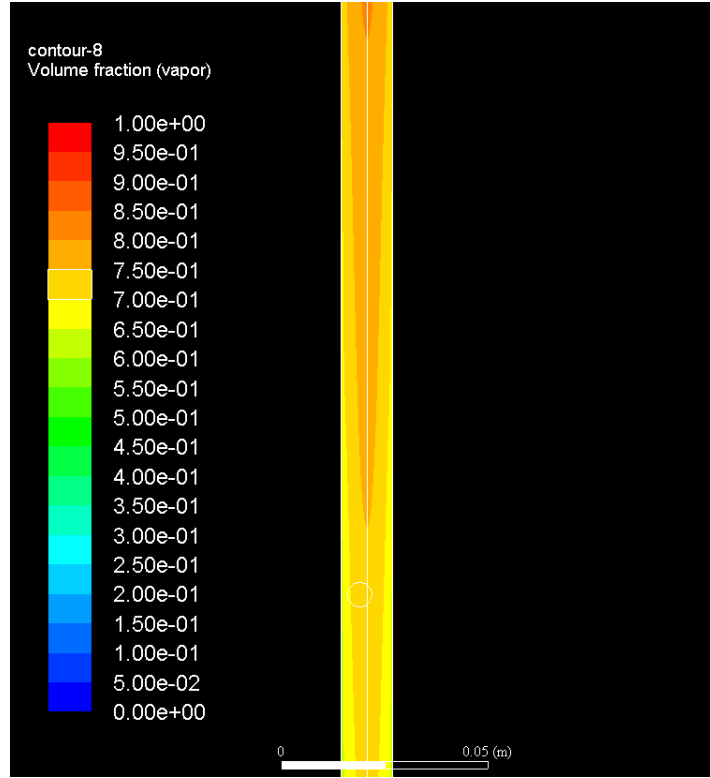


Figure 4: The field distribution of vapor volume fraction.

The comparison against experiment of the vapor volume fraction with the inlet mass flux of 1750 kg/(m²s) is shown in Figure 5. As well as in the former case, the maximum computation error is reported at the outlet boundary and has a value of 5.82%.

In comparison to Figure 3, one can notice how the error is decreasing in the case of the lower mass flux. Thus, in the case with inlet mass flux $750 \text{ kg}/(\text{m}^2 \text{ s})$ the minimum error is 2.73%. On the other hand, in the simulation with the higher mass flux, the smallest error is 5.41% what is slightly less than the maximum value reported at the domain's outlet.

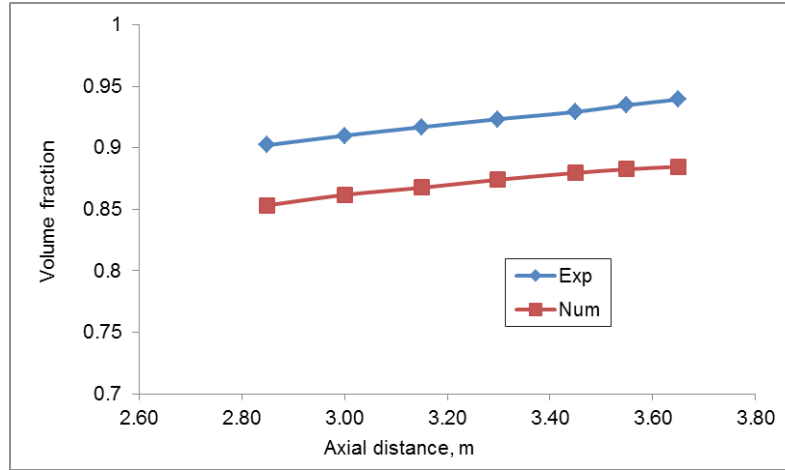


Figure 5: Axial void fraction distribution in the case with the mass flux $1750 \text{ kg}/(\text{m}^2 \text{ s})$.

5 Conclusion

A numerical model for computation of annular flow boiling in a vertical heated pipe has been developed using Eulerian two-fluid model. An emphasis is put on capturing the annular flow characteristics, i.e. the occurrence of liquid film adjacent to wall and a vapor core. To accomplish this, the correlations for lift force coefficient and interfacial area density were implemented within the framework of commercial CFD code ANSYS Fluent 18.1 via user-defined functions. A comparison with the experimental data has shown the reliability of the developed model.

References

- [1] S.-J. Yoon, G. Agostinelli, E. Baglietto. Assessment of multiphase CFD with zero closure model for boiling water reactor fuel assemblies. In: *17th International Topical Meeting on Nuclear Reactor Thermal Hydraulics (NURETH 17)*, Xi'an, China, 2017.
- [2] C. Adamsson. Measurements of Film Flow Rate in Heated Tubes with Various Axial Power Distributions. *PhD Thesis*, KTH Sweden, 2006.
- [3] ANSYS Fluent 18.2. Theory Guide. 2017.
- [4] C. Geuzaine, J.-F. Remacle. Gmsh: a three-dimensional finite element mesh generator with built-in pre- and post-processing facilities. *International Journal for Numerical Methods in Engineering*, Volume **79**, Issue 11, pages 1309-1331, 2009.

- [5] A. Galović, B. Halasz, I. Boras. *Toplinske tablice*. Fakultet strojarstva i brodogradnje, 2008.
- [6] S.N. Fincher. Numerical Simulations of Boiling in Dielectric Fluid Immersion Cooling Scenarios of High Power Electronics. *Master of Science Thesis*, Auburn University, 2014.
- [7] ANSYS, Inc. Tutorial: Modeling Nucleate Boiling Using ANSYS FLUENT. 2017.
- [8] A. Rohatgi. WebPlotDigitizer, version 3.9. 2015.